Organic Compounds in the Environment

Two-Dimensional Model Simulation of 1,3-Dichloropropene Volatilization and Transport in a Field Soil

D. Wang,* J. A. Knuteson, and S. R. Yates

ABSTRACT

A modeling study was conducted to simulate 1,3-dichloropropene (1,3-D) emission and concentration distribution in soil profiles when the chemical was applied with subsurface drip irrigation with reduced rate. The purpose was to evaluate the effect on emission reduction as compared with conventional shank injection application. To compare with field measurements, simulated scenarios included a shallow drip application at 2.5 cm, covered with a polyethylene film; a deep drip application at 20.3 cm with bare soil surface; and a conventional shank injection at 30.5 cm with a regular application rate. A convective and diffusive two-dimensional model was used to simulate the simultaneous transport of 1,3-D in both liquid and gaseous phases. Diurnal variations of soil temperature were predicted to calculate 1,3-D diffusion coefficient and the Henry's constant. Predicted 1,3-D emissions compared well with field measurements for the shallow and deep drip irrigation treatments. The model simulation underpredicted 1,3-D emission in the shank injection plot, where other transport mechanisms such as gas phase convection likely occurred during and immediately after application. Results from the modeling study indicate that computer simulation can be used effectively to study the environmental fate and transport of 1,3-D under conditions where vapor phase diffusion and liquid phase convection are the dominant transport mechanisms. Applying 1,3-D with subsurface drip irrigation appeared to be useful for emission reduction.

Accurate characterization of fate and transport of volatile organic chemicals such as 1,3-D is important to determine environmental air pollution from anthropogenic contaminant sources (Singh et al., 1992). Adverse environmental effects occur when the volatile compounds reach the atmosphere by volatilization from the soil surface (Spencer and Cliath, 1973). The dynamics of chemical volatilization are strongly controlled by the subsurface transport and ambient environmental conditions, which may be described with process-based transport models (Jury et al., 1983). Because a volatile chemical will have a significant portion in the vapor phase, its fate and transport in a porous media would simultaneously occur in both the gaseous and liquid phases (Amali et al., 1996). Adsorption and desorption with the solid phase or soil particles would make the transport process more transient (Petersen et al., 1996). Temperature also is found to affect the transport parameters, especially for the vapor phase diffusion and vapor-to-liquid phase partition coefficients for methyl bromide (MeBr) (Wang et al., 1997a, 1998a).

D. Wang and S.R. Yates, U.S. Salinity Laboratory, 450 West Big Springs Road, Riverside, CA 92507-4617; and J.A. Knuteson, Dow AgroSciences, 9330 Zionsville Road, Indianapolis, IN 46268-1053. Received 29 March 1999. *Corresponding author (dwang@ussl.ars.usda.gov).

Published in J. Environ. Qual. 29:639–644 (2000).

It has been shown that 1,3-D is a very effective fumigant that controls many soil-born pests and plant pathogens (Noling and Becker, 1994) and is being considered as a potential alternative to MeBr. However, current agricultural use of 1,3-D in California and other regions of the USA is restricted to very low rates and under restricted conditions because of observed large gas emission losses. Chen et al. (1995) reported that about 25 to 50% of the applied 1,3-D could be lost to the atmosphere by volatilization when applied with conventional shank injection. To reduce 1,3-D volatilization loss, an alternative management method is to apply 1,3-D with subsurface drip irrigation at a reduced rate (a fraction of the shank injection). Subsurface drip irrigation has an advantage over the shank injection since the drip tapes may be installed prior to 1,3-D application and the compound is pre-mixed or diluted in water to concentrations less than the solubility. In the shank injection, however, significant amounts of 1,3-D may be lost because of direct evaporation of 1,3-D liquid through the shank fractures during or immediately after application, such as in MeBr (Yates et al., 1997).

This modeling study was designed to simulate 1,3-D fate and transport in soil and volatilization into the atmosphere when the chemical was applied with either shank injection or drip irrigation at two different depths. The overall objective was to reduce 1,3-D emission losses with subsurface drip irrigation, which was achieved by comparing different application scenarios. Model predictions also were compared with field measurements using independently obtained input parameters.

MATERIALS AND METHODS

Model Description

A generic two-dimensional finite element code CHAIN_2D (Simunek and van Genuchten, 1994) was used for simulating 1,3-D fate and transport in the soil and volatilization into the atmosphere. The governing equation for describing 1,3-D transport in both gaseous and liquid phases can be written as:

$$\frac{\partial \theta C_L}{\partial t} + \frac{\partial \rho C_s}{\partial t} + \frac{\partial a_s C_g}{\partial t} = \theta D_L \frac{\partial}{\partial x}\left[\frac{\partial C_L}{\partial z}\right] + a_s D_g \frac{\partial}{\partial x}\left[\frac{\partial C_g}{\partial z}\right] - \frac{\partial q C_L}{\partial z} - \mu_L \theta C_L - \mu_s \rho C_s \quad [1]$$

where C_L, C_s, and C_g are 1,3-D concentrations in the soil in liquid (M L^{-3}), solid (M M^{-1}), and gaseous (M L^{-3}) phases,

Abbreviations: 1,3-D, 1,3-dichloropropene; MeBr, methyl bromide; PE, polyethylene.

respectively; θ is soil volumetric water content ($L^3\ L^{-3}$); ρ is soil bulk density ($M\ L^{-3}$); a_s is soil air content ($L^3\ L^{-3}$); D_L and D_g are 1,3-D effective diffusion coefficients in liquid and gaseous phases ($L^2\ T^{-1}$), respectively; q is volumetric liquid flux density ($L\ T^{-1}$); μ_L and μ_s are first-order degradation rate constants for 1,3-D in liquid and solid phases (T^{-1}), respectively; t is time (T); and x and z are lateral and vertical distances (L).

The liquid flux density (q), calculated with the Richards' equation, determines the rate of 1,3-D convective transport in the liquid or solution phase. The model assumes nonequilibrium interaction between the solution and adsorbed concentrations, and equilibrium interaction between the solution and gaseous concentrations. A linear relationship was used for 1,3-D partition between the three phases. Degradation of 1,3-D was considered in the solution and adsorbed phases, but not in the air, using a first order decay having the same rate constant.

Field Measurements

A field experiment was conducted, with direct measurements of 1,3-D gas emission and concentration distribution in the soil, to provide comparisons with the model simulations. The field treatments were: (i) shallow drip application at 2.5 cm, covered with a polyethylene (PE) film; (ii) deep drip application at 20.3 cm with bare soil surface; and (iii) shank injection at 30.5 cm with bare soil surface. The soil was an Arlington fine sandy loam (coarse-loamy, mixed, thermic Haplic Durixeralf). Application of 1,3-D with the irrigation water for the two drip treatments was at a 4.1 $cm^3\ min^{-1}\ m^{-1}$ rate and lasted for 6.7 h. Water flow was continued for an additional 1.5 h after 1,3-D injection to flush out residual 1,3-D. The final amount of 1,3-D applied for the two drip treatments was 4.7 g m^{-2} (47 kg ha^{-1}). In the shank injection treatment, 1,3-D application lasted only about 5 min to inject to the subsurface soil pure 1,3-D liquid at a 11.2 g m^{-2} (112 kg ha^{-1}) rate.

Replicated flux chambers were placed over the top, side, and furrow of the field beds of each application treatment to measure 1,3-D emission flux density. Ambient air from 10 m outside the field and upwind was continuously drawn, with 5-cm diameter aluminum pipes, through each chamber with a vacuum system. The air passing through the chambers was subsampled every 3 h for analysis of 1,3-D concentrations and determination of emission flux density. Activated coconut charcoal tubes were used to absorb 1,3-D from the air stream at chamber outlets.

Soil–air samplers were installed at several depths to 1 m below the bed center of each treatment. They were used for measurements of 1,3-D gas concentration distribution. To prevent chemical adsorption, small Teflon tubing was used in the two drip treatments for 1,3-D gas sampling. The tubing was installed before 1,3-D application. In the shank treatment, small rigid stainless steel tubing was pushed into the soil right after 1,3-D injection, without soil excavation. Except for the first sampling sequence (where 20 cm^3 was taken), 40 cm^3 soil air from each sampling point was drawn through the same type of activated charcoal tubes used for emission measurements. For both the emission and soil gas samples, total 1,3-D mass from each tube was analyzed with a Hewlett–Packard 5890 gas chromatograph (Palo Alto, CA).

Model Application and Parameterization

The initial 1,3-D concentration in the soil profile is controlled by the amount and method of application. For shank injection, an instantaneous line source is added in the two-dimensional domain (across the field rows) and can be described as:

$$C_{L,g}(x, z, 0) = C_o(x_i, z_i) \quad [2]$$

and

$$C_{L,g}(x, z, 0) = 0\ (x \neq x_i, z \neq z_i) \quad [3]$$

where C_o is the 1,3-D concentration at the source ($M\ L^{-3}$) and x_i and z_i specify the source location in the soil profile. Because 1,3-D was injected 30.5 cm below bed center with a row spacing of 102 cm, z_i = 30.5 cm and x_i is centered around 51 cm extending half the length of shank knife in both directions.

Similar to input procedures used in Wang et al. (1997b) for chemical application with drip irrigation, 1,3-D was added in the two-dimensional domain as a flux input and is described as:

$$Q = Q_o(t = 0 - t_o) \quad [4]$$

and

$$C_L = \begin{cases} C_i & (t = 0 - t_i) \\ 0 & (t = t_i - t_o) \end{cases} \quad [5]$$

where Q or Q_o is the irrigation rate ($L^3\ T^{-1}\ L^{-1}$), t_o is the total duration of drip irrigation (T), and t_i is 1,3-D injection duration (T). To compare with the field experiment, 1,3-D was applied at 2.5- and 20.3-cm depths and called shallow and deep drip, respectively.

To simulate 1,3-D emission, the model used a volatilization boundary condition of the form:

$$J = \frac{D_g}{d}(C_g - C_{atm}) \quad [6]$$

where J is 1,3-D emission flux density ($M\ L^{-2}\ T^{-1}$), D_g and C_g are previously defined in Eq. [1], C_{atm} is the 1,3-D concentration above the surface boundary layer ($M\ L^{-3}$), and parameter d is the boundary layer thickness (L) for characterizing the resistance to 1,3-D transport across the soil–atmosphere interface. When the soil surface is covered with plastic film, parameter d is attributed primarily from resistance from the film and is found to be highly temperature dependent (Wang et al., 1997a). Because of symmetry, a zero flux boundary condition

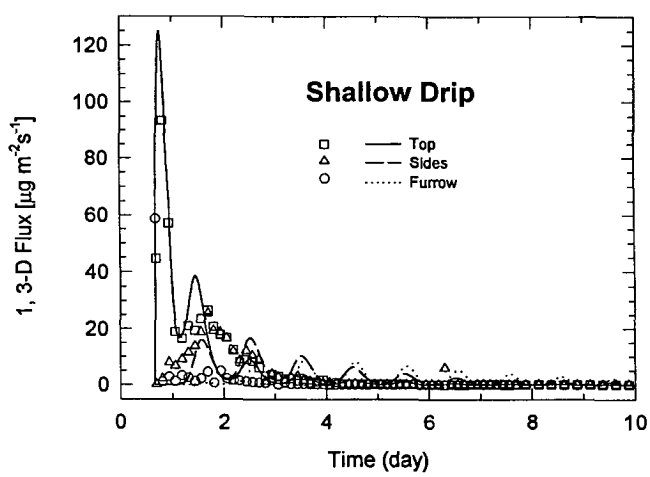

Fig. 1. Volatilization flux density of 1,3-dichloropropene from field beds of the shallow drip irrigation plot covered with a polyethylene film. Symbols are measured values and lines are simulated fluxes.

was used for the sides of the simulation domains. A unit flux boundary condition was used for the bottom boundary.

The gaseous phase diffusion coefficient (D_g), the modified Henry's constant ($K_h = C_g / C_L$), and the boundary layer thickness (d) are all highly temperature dependent (Wang et al., 1997a). To account for temperature effect on 1,3-D transport and volatilization, a generic equation similar to the Arrhenius equation is used in model simulation to calculate apparent D_g, K_h, and d for each time increment. The equation can be written as:

$$\beta(T_a) = \beta_r^{Tr} \exp\left(\frac{T_r - T_a}{RT_aT_r}E_a^{\beta}\right) \quad [7]$$

where β (T_a) describes a temperature-dependent parameter such as D_g or K_h; β_r^{Tr} is the reference value for parameter β at a reference temperature (T_r); $E_a^{\beta r}$ is the activation energy for parameter β (J mol^{-1}); T_a is the apparent soil or air temperature (K); T_r is the reference temperature (K); and R is the universal gas constant (8.314 J mol^{-1} K^{-1}).

The temperature dependent model parameters were obtained as follows: for T_r = 20°C, K_h^{Tr} = 0.0446, and E_a^{kh} = 4.3207 × 10^4 J mol^{-1} (fitted from Fig. 1 of Leistra, 1970); D_g^{Tr} = 0.0832 cm^2 s^{-1} and E_a^{Dg} = 4.511 × 10^3 J mol^{-1} (calculated from Eq. [5] of Wang et al., 1997a and fitting to Eq. [7] of this paper); d^{Tr} = 135 cm and E_a^d = −2.1212 × 10^3 J mol^{-1} (converted from measurements reported in Wang et al., 1999) for the plastic-covered shallow drip treatment. The boundary layer thickness (d) for the deep drip and shank injection treatments was 0.5 cm since the volatilization was through the bare soil surface (Jury et al., 1983) and it also was assumed to be temperature independent, or E_a^d = 0. According to data from van Dijk (1980), the first-order degradation rate constant was 0.1392 d^{-1} for 1,3-D in both the liquid and solid phases, or $\mu_L = \mu_s$. The activation energy also was the same (E_a^{μ} = 4.3551 × 10^4 J mol^{-1}) in both phases with no degradation in the gas phase. The liquid to solid phase adsorption coefficient was 0.3 cm^3 g^{-1} and was independent of temperature (Wolt et al., 1993). Other temperature-independent parameters include soil hydraulic properties and bulk density. Functions describing water flow in the model required five parameters, θ_r, θ_s, α, n, and K_s. Of these, θ_r and θ_s represent residual and saturated volumetric soil water content; α and n are characteristic hydraulic parameters of the soil, and K_s is the hydraulic conductivity at saturation. Values for these parameters for this samdy loam soil were found in Wang et al. (1998b) as: θ_r = 0.0768, θ_s = 0.3705, α = 0.3571 cm^{-1}, n = 1.3731, and K_s = 34.0 cm d^{-1}. Soil bulk density was measured from replicated field gravimetric samples and was found to be 1.60 g cm^{-3} for the two drip treatments and 1.44 g cm^{-3} for the shank injection.

RESULTS AND DISCUSSION

Shallow Drip Irrigation

In the shallow drip irrigation, the measured 3-h average emission flux density reached a maximum of 93 μg m^{-2} s^{-1} from the bed top location right after 1,3-D application (Fig. 1). The model simulated an instantaneous maximum flux of 125 μg m^{-2} s^{-1} at the same location and time as the maximum occurred in the field measurement. Because of the temperature effect on 1,3-D diffusion rate, partitioning into the vapor phase, and permeability of the PE tarp, the simulated volatilization showed strong diurnal cyclic behavior with large fluxes occurring near solar noon and low values near midnight. The measurements also showed the cyclic behavior during the first 2 d after 1,3-D application, after which the absolute flux density became very small. Simulation at the bed sides and furrow locations slightly underpredicted the emission flux density during the first 2 d and overpredicted the flux after Day 2. Overall, the model simulation predicted that 68.7% of the applied 1,3-D was lost via atmospheric emission, while the measurements indicated that 66.3% was lost (Table 1). Therefore, the model closely simulated 1,3-D volatilization when the chemical was applied with drip irrigation at 2.5 cm and the surface covered with a PE film. Over time, the model also closely predicted the emission dynamics, as the predicted cumulative emission losses compared well with the measurements (except at 0.63 and 0.78 d after application). With the model, we predicted also the amount of 1,3-D that had been degraded

Table 1. Partition of 1,3-D between percent emitted, degraded, and remaining in the soil at selected times after application with drip irrigation.

Elapsed time	Simulated emission	Measured emission	Simulated degradation	Remaining in the soil	Numerical mass balance error
days			%		
Shallow Drip Application†					
0.00	0.0	0.0	0.0	100.0	0.0
0.63	27.1	5.2	7.1	65.3	0.5
0.78	34.4	13.5	8.9	56.3	0.4
1.40	49.7	30.3	14.1	36.3	0.1
2.31	58.2	54.4	19.3	24.9	2.4
3.32	62.3	62.6	23.5	17.8	3.6
9.78	68.1	66.0	33.9	3.5	5.5
29.8	68.7	66.3	36.9	<0.1	5.7
Deep Drip Application‡					
0.00	0.0	0.0	0.0	100.0	0.0
0.64	5.3	0.2	8.8	85.3	0.6
0.79	9.4	3.7	11.1	78.9	0.6
1.79	28.3	35.0	23.0	49.7	1.0
2.31	34.0	43.4	27.3	41.1	2.4
3.32	40.8	52.1	34.0	29.4	4.2
9.78	50.6	56.6	50.8	5.6	7.0
29.8	51.6	56.8	55.6	<0.1	7.2

† Shallow drip at 2.5 cm depth with surface covered with polyethylene film.
‡ Deep drip at 20.3 cm depth, bare soil.

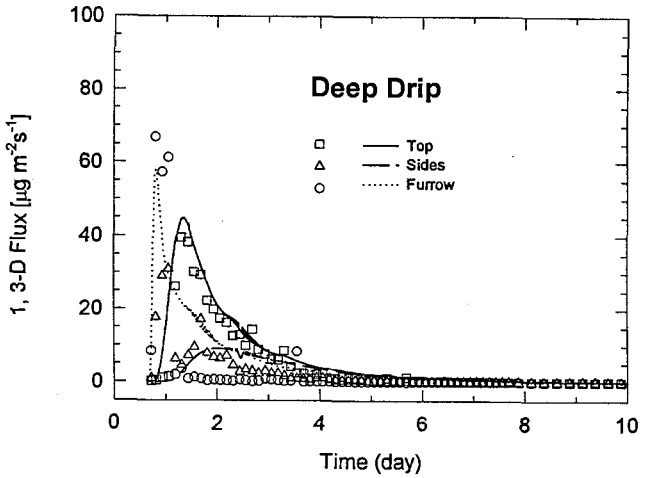

Fig. 2. Volatilization flux density of 1,3-dichloropropene from field beds of the deep drip irrigation plot with bare soil surface. Symbols are measured values and lines are simulated fluxes.

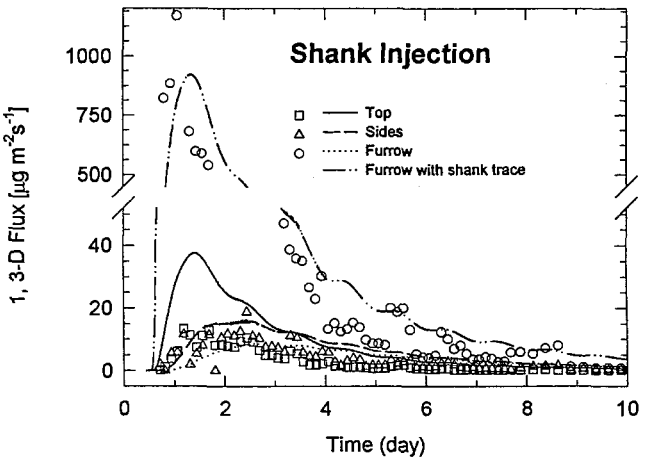

Fig. 3. Volatilization flux density of 1,3-dichloropropene from field beds of the shank injection plot with bare soil surface. Symbols are measured values and lines are simulated fluxes.

at selected times after application. At the end of the simulation run, about 37% had been lost to soil degradation. The simulation is reasonable because <6% numerical mass balance error was produced.

Deep Drip Irrigation

When 1,3-D was applied to 20.3 cm depth with the drip irrigation, the maximum emission flux density occurred from the furrow location and reached a maximum value of 67 μg m^{-2} s^{-1} (Fig. 2). The model prediction of the maximum flux was 58 μg m^{-2} s^{-1} for the same field location. Emission from the bed top reached a maximum of 39 μg m^{-2} s^{-1} at about 10 h after the deep drip application. It appears that 1,3-D reached the bed furrows before reaching the bed top after application with the drip irrigation water. This is possible because the transport to the bed top was against gravity and the coupled convective flow with the irrigation water had to overcome the gravity force. For the lateral movement to the furrows, however, both convective flow by water potential gradient and gas diffusion would drive the chemical to the soil surface in the bed furrows. In addition to losses from both the top and furrows of the field beds, significant emission loss also occurred from the sides of the field beds, where the maximum flux was 9.6 μg m^{-2} s^{-1} and persisted for about 8 h. The model simulation closely predicted emission from all three bed locations. Compared with the shallow drip plot, neither the model prediction nor the field measurements showed any diurnal variation in the emission flux density. This is caused by the absence of plastic film since the temperature effect on the permeability of the PE film was not a factor in the deep drip application. The model simulation predicted a total of 51.6% emission loss, while the field measurements showed that 56.8% was lost via atmospheric emission (Table 1). This is a significant reduction (10 to 17%) from the shallow drip application. According to the predictions, the total 1,3-D mass lost by volatilization was 3.2 and 2.4 g m^{-2} for the shallow and deep drip, respectively. However, the small dosage was sufficient in controlling soil nematodes (Wang and Yates, 1999). A maximum of about 7% numerical mass balance error was produced during the simulation and the model predicted that 55.6% of the 1,3-D would have been lost to soil degradation.

Shank Injection

Extremely high flux density (about 1150 μg m^{-2} s^{-1}) was observed from the furrow locations when 1,3-D was applied with slanted shanks at 30.5 cm depth (Fig. 3). If the soil is uniform, the predicted maximum flux was only 38 μg m^{-2} s^{-1} and should occur on the top of the field beds. The model simulation predicted a total of about 40% (or 4.5 g m^{-2}) of the shank-injected 1,3-D being lost to atmospheric emission (Table 2). However, the field measurements indicated that over 90% (or >10 g m^{-2}) was lost by emission. In either case, more 1,3-D was lost than in the subsurface drip irrigation treatments. The most probable cause for the underprediction was that the slanted shanks created a fracture during the injection and a significant amount of 1,3-D was lost through the preferential pathways during and right after the shank injection. To simulate such a nonuniform soil condition, a narrow zone of low density soil along the shank trace was used in a modified two-dimensional simulation domain. This zone of unconsolidated soil was used to simulate the shank fractures to determine the effect of preferential diffusion flow on 1,3-D emission losses. Holding all other parameters the same, the predicted maximum flux did occur in the furrow location and reached a maximum value of about 920 μg m^{-2} s^{-1}. The predicted overall emission with the nonuniform soil was only about 50% of the applied amount, still much less than the field measurements. It is likely that other transport mechanisms such as convective gas transport might have contributed to the redistribution and emission in shank injection. Small pressure gradients (positive) between the highly concentrated 1,3-D source and the soil surface could create large flux values at early times and the low resistance to preferential pathway could allow significant emission losses.

Table 2. Partition of 1,3-D between percent emitted, degraded, and remaining in the soil at selected times after shank injection at 30.5 cm depth.

Elapsed time	Simulated emission	Measured emission	Simulated degradation	Remaining in the soil	Numerical mass balance error
days			%		
Simulation with Uniform Soil					
0.00	0.0	0.0	0.0	100.0	0.0
1.20	8.2	35.5	19.6	71.9	0.2
2.12	18.1	73.3	30.4	53.3	1.8
3.63	27.8	89.8	35.4	34.4	2.4
4.63	31.5	93.0	48.2	26.2	6.0
5.63	33.9	95.2	52.6	20.3	6.8
9.78	37.9	98.4	62.5	7.6	8.0
30.03	39.5	98.9	69.1	<0.1	8.7
Simulation with Nonuniform Soil†					
0.00	0.0	0.0	0.0	100.0	0.0
1.20	12.1	35.5	19.6	69.7	1.4
2.12	23.7	73.3	29.9	50.1	3.7
3.63	34.0	89.8	41.2	31.7	6.9
4.63	37.9	93.0	46.5	25.7	10.2
5.63	40.7	95.2	50.9	21.1	12.7
9.78	46.4	98.4	62.2	9.8	18.3
30.03	49.4	98.9	72.7	0.3	22.4

† Nonuniform soil consisted of a shank trace with reduced soil bulk density.

Concentration in Soil

Consistent with the emission predictions, predicted 1,3-D gas concentrations in the soil profile compared reasonably well with the direct soil air measurements in the shallow drip plot (Fig. 4). At 0.63 and 0.78 d after 1,3-D application, the model slightly underpredicted the gas concentration due to the overprediction in the emission fluxes. The predicted maximum gas concentration, however, was very similar to the measurements, reaching about 8.4 and 5.2 μg cm^{-3} for 0.63 and 0.78 d, respectively. At longer times, the predicted concentrations became closer to the field measurements. In the deep drip treatment, the predicted 1,3-D concentrations matched well with the measured values (Fig. 5). At 0.64 and 0.79 d after application, the predicted peak concentrations appeared to be closer to the soil surface or subjected to less downward movement than the measured values. At longer times after application, the model slightly overpredicted 1,3-D concentrations in the soil profile. This is consistent with the flux predictions since a small underprediction was found in the total cumulative emission for the deep drip treatment (Table 1). Significant overprediction was found for 1,3-D gas concentrations in the soil profile when the chemical was applied with the shank injection method (Fig. 6). Although the center mass remained at about 30 to 40

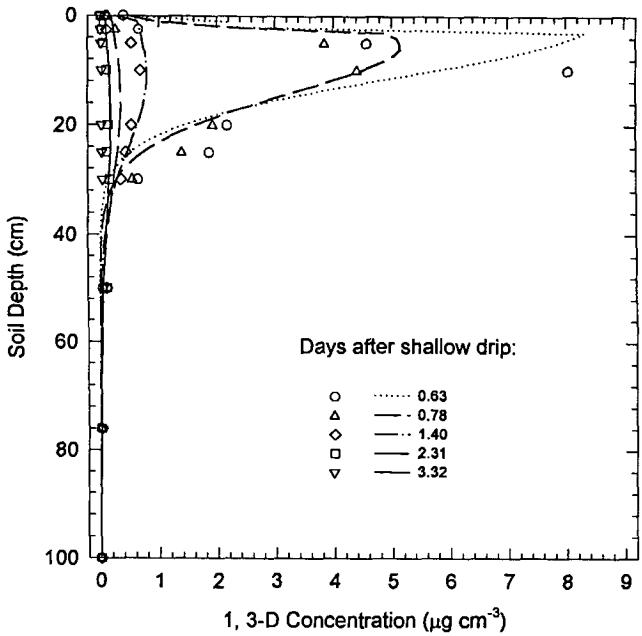

Fig. 4. Concentrations of 1,3-dichloropropene in soil air directly below the bed center of the shallow drip irrigation plot. Symbols are direct field measurements and lines are simulated concentrations in the soil profile.

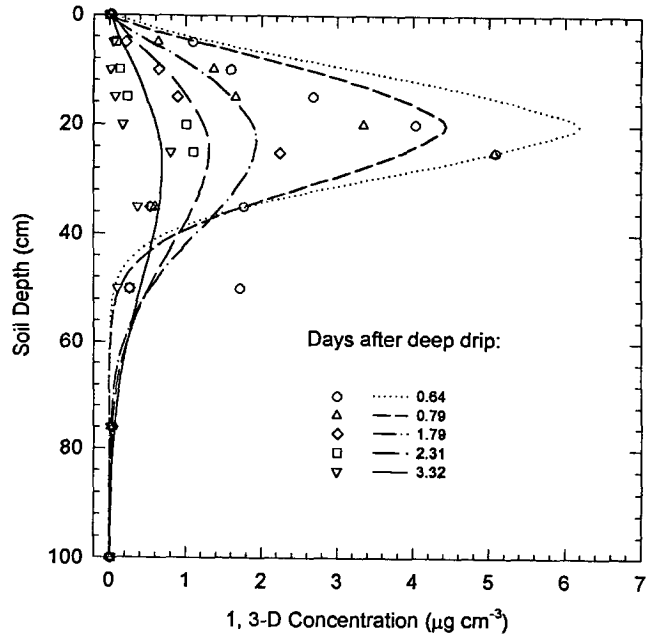

Fig. 5. Concentrations of 1,3-dichloropropene in soil air directly below the bed center of the deep drip irrigation plot. Symbols are direct field measurements and lines are simulated concentrations in the soil profile.

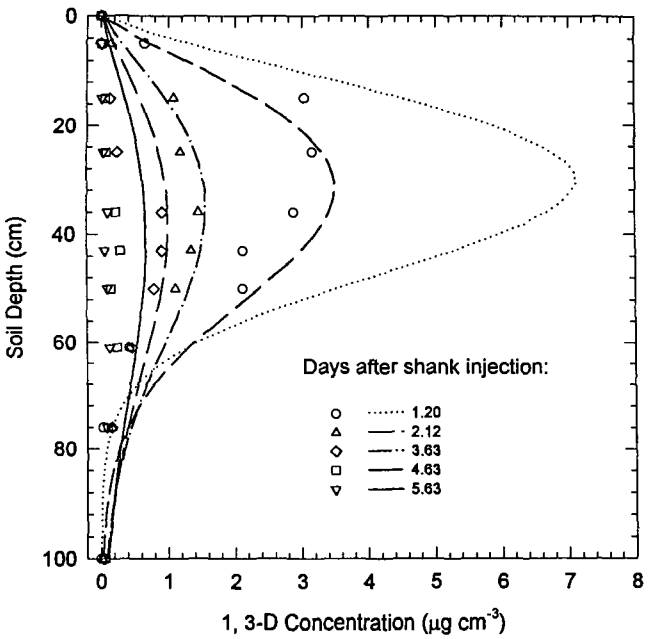

Fig. 6. Concentrations of 1,3-dichloropropene in soil air directly below the bed center of the shank injection plot. Symbols are direct field measurements and lines are simulated concentrations in the soil profile.

cm, the predicted absolute concentration values were about twice the actual field measurements. This would verify that the measured total emission losses should be twice the predicted total emission (Table 2). The results suggest that other transport mechanisms such as vapor phase convection may be needed in predicting 1,3-D volatilization during shank injection.

CONCLUSIONS

Fate and transport of 1,3-D in soil fumigation was simulated with a two-dimensional multiphase solute transport model. Less 1,3-D mass loss was found for application with drip irrigation than shank injection. Compared with the field measurements, model simulation predicted well the emission flux density and soil gas concentrations when 1,3-D was applied with drip irrigation. The model underpredicted emission when the chemical was applied with shank injection. It appears that computer modeling can be used effectively to study the environmental fate and transport of 1,3-D under conditions where gas diffusion and liquid phase convection are dominant.

REFERENCES

Amali, S., D.E. Rolston, and T. Yamaguchi. 1996. Transient multicomponment gas-phase transport of volatile organic chemicals in porous media. J. Environ. Qual. 25:1041–1047.

Chen, C., R.E. Green, D.M. Thomas, and J.A. Knuteson. 1995. Modeling 1,3-dichloropropene fumigant volatilization with vapor-phase advection in the soil profile. Environ. Sci. Technol. 29:1816–1821.

Jury, W.A., W.F. Spencer, and W.J. Farmer. 1983. Behavior assessment model for trace organics in soil: I. Model description. J. Environ. Qual. 12:558–564.

Leistra, M. 1970. Distribution of 1,3-dichloropropene over the phases in soil. J. Agric. Food Chem. 18:1124–1126.

Noling, J.W., and J.O. Becker. 1994. The challenge of research and extension to define and implement alternatives to methyl bromide. J. Nematol. 26:573–586.

Petersen, L.W., Y.H. El-Farhan, P. Moldrup, D.E. Rolston, and T. Yamaguchi. 1996. Transient diffusion, adsorption, and emission of volatile organic vapors in soils with fluctuating low water contents. J. Environ. Qual. 25:1054–1063.

Simunek, J., and M. Th. van Genuchten. 1994. The CHAIN_2D code for simulating the two-dimensional movement of water, heat, and multiple solutes in variably-saturated porous media. Res. Rep. No. 136, Version 1.1. U.S. Salinity Laboratory, USDA-ARS, Riverside, CA.

Singh, H.B., L. Salas, W. Viezee, B. Sitton, and R. Ferek. 1992. Measurement of volatile organic chemicals at selected sites in California. Atmos. Environ. 26:2929–2946.

Spencer, W.F., and M.M. Cliath. 1973. Pesticide volatilization as related to water loss from soil. J. Environ. Qual. 2:284–289.

Van Dijk, H. 1980. Dissipation rates in soil of 1,2-dichloropropane and 1,3- and 2,3-dichloropropenes. Pestic. Sci. 11:625–632.

Wang, D., and S.R. Yates. 1999. Spatial and temporal distributions of 1,3-dichloropropene in soil under drip and shank application and implications for pest control efficacy using concentration–time index. Pestic. Sci. 55:154–160.

Wang, D., S.R. Yates, and F.F. Ernst. 1998b. Determining soil hydraulic properties using tension infiltrometers, time domain reflectometry, and tensiometers. Soil Sci. Soc. Am. J. 62:318–325.

Wang, D., S.R. Yates, and J. Gan. 1997a. Temperature effect on methyl bromide volatilization in soil fumigation. J. Environ. Qual. 26:1072–1079.

Wang, D., S.R. Yates, J. Gan, and W.A. Jury. 1998a. Temperature effect on methyl bromide volatilization: Permeability of plastic cover films. J. Environ. Qual. 27:821–827.

Wang, D., S.R. Yates, J. Gan, and J.A. Knuteson. 1999. Atmospheric volatilization of methyl bromide, 1,3-dichloropropene, and propargyl bromide through two plastic films: Transfer coefficient and temperature effect. Atmos. Environ. 33:401–407.

Wang, D., S.R. Yates, J. Simunek, and M. Th. van Genuchten. 1997b. Solute transport in simulated conductivity fields under different irrigations. J. Irrig. Drain. Eng. 123:336–343.

Wolt, J.D., D.L. Holbrook, F.R. Batzer, J.L. Balcer, and J.R. Peterson. 1993. Dynamics of nematicide distribution and degradation in soil subjected to long-term pineapple culture. Acta Hortic. 334:361–371.

Yates, S.R., D. Wang, F.F. Ernst, and J. Gan. 1997. Methyl bromide emissions from agricultural fields: Bare-soil, deep injection. Environ. Sci. Technol. 31:1136–1143.